Structural Changes in Lamellar Diblock Copolymer Thin Films upon Swelling in Nonselective Solvents

ARTICLE *in* MACROMOLECULES · JULY 2013

Impact Factor: 5.8 · DOI: 10.1021/ma400810u

Macromolecules

Article

pubs.acs.org/Macromolecules

Structural Changes in Lamellar Diblock Copolymer Thin Films upon Swelling in Nonselective Solvents

Andrey A. Rudov,[†,‡] Elena S. Patyukova,[†] Irina V. Neratova,[§,∥] Pavel G. Khalatur,[§] Dorthe Posselt,[⊥] Christine M. Papadakis,[#] and Igor I. Potemkin*[,†,‡,§]

[†]Physics Department, Lomonosov Moscow State University, Moscow 119991, Russian Federation

[‡]Institute of Interactive Materials Research, DWI an der RWTH, Aachen 52056, Germany

[§]Institute for Advanced Energy Related Nanomaterials, University of Ulm, D-89069 Ulm, Germany

[∥]Leibniz-Institut für Polymerforschung Dresden e.V., 01069 Dresden, Germany

[⊥]IMFUFA, Department of Science, Systems and Models, Roskilde University, P.O. Box 260, 4000 Roskilde, Denmark

[#]Technische Universität München, Physik-Department, Physik weicher Materie, 85748 Garching, Germany

ABSTRACT: Using dissipative particle dynamics simulations, we study the swelling of lamellae-forming diblock copolymer films in a nonselective solvent. Both the parallel and the perpendicular orientations of lamellae in the film are studied. The swelling of the film with parallel lamellae is accompanied by an increase of their number. In doing so, the lamellar thickness reveals nonmonotonous behavior: affine growth (low degree of solvent uptake) is succeeded by a decrease in thickness (high degree of solvent uptake). Whereas the first regime reflects a finite size (film thickness) effect, the decrease is a more common effect, which is also valid for perpendicular lamellae, and is due to shrinkage of the diblock copolymers due to the shielding of unfavorable AB contacts by the solvent molecules. The film swelling leads to an increase of the number of perpendicular lamellae as well. However, such an increase is only possible if the film at first is dissolved and then condensed absorbing a certain amount of solvent. Otherwise, splitting of the lamellae requires a large-scale mass transport which is realizable neither in modeling nor in experiment. Instead of splitting, the perpendicular lamellae can tilt upon swelling. This process is much faster and satisfies the space-filling condition at the thinning of the lamellae. That is why tilted lamellae are often observed in experiments and computer simulations. We demonstrate also that the distribution of the absorbed solvent in the film is inhomogeneous with a maximum at the AB interfaces. The kinetics of the parallel lamellae swelling is compared with experimental data.

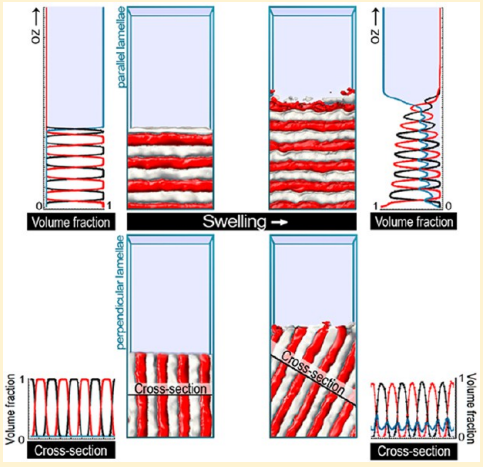

INTRODUCTION

Control of nanodomains orientation in block copolymer films is one of the key problems for many applications including growth of ultrahigh-density nanowire arrays for storage media,[1] manufacturing of organic photovoltaic devices with a well-developed interfacial area to efficiently perform charge collection and transfer to electrodes,[2] manufacturing of dielectric reflectors,[3] sensors,[4] etc. There are a number of tools allowing control of the nanodomain orientation. However, the most attractive among them is a spontaneous domain orientation which is driven by relaxation of the system to the equilibrium state. It has been demonstrated that the perpendicular domain orientation in diblock copolymer films corresponds to equilibrium, if the interactions of both blocks with the film surfaces are similar[5,6] (the so-called neutral surfaces). To obtain such similarity, the surfaces can be modified by random AB copolymers consisting of monomer units identical to the ones of the diblock copolymers.[7] In addition to the various interaction parameters, the film thickness plays an important role: reliable stability of perpendicular nanodomains on neutral surfaces is achieved only for thinner films.[6] Preferential interaction of one of the components of the diblock copolymer with the surfaces is primarily responsible for the parallel orientation of the nanodomains.[5,6] In some cases, the molecular weight of diblock copolymers can control the orientations. For example, symmetric high-molecular-weight PS-*b*-PB diblock copolymers on a silicon oxide substrate form perpendicular lamellae, whereas short enough diblock copolymers exhibit layered structures.[8,9] The physical reason for such an orientation effect in the strong segregation regime is related to the dependence of the interdomain surface tension coefficient on the length of the macromolecules.[9] In the case of patterned substrates, selective interactions of A and B blocks with the patterns can promote

Received: April 19, 2013
Revised: June 7, 2013
Published: July 3, 2013

   dx.doi.org/10.1021/ma400810u | *Macromolecules* 2013, 46, 5786−5795

the perpendicular domain orientation, if the period of the pattern is commensurable with the bulk period of the block copolymer.[10−13] Association of liquid-crystalline groups with one of the blocks of a diblock copolymer can also lead to the perpendicular orientation of amorphous nanodomains due to selective interactions of the groups with the substrate.[14,15] It has been shown recently that physical attachment of the ends of a diblock copolymer to a substrate and variation of the "grafting" density of the diblock copolymers in such a planar brush can control the domain orientation.[16] In particular, a parallel double layer or (depending on copolymer composition) parallel cylinders are stable at low enough grafting density. Surprisingly, the cylinders are transformed into vertical "stalactites" or "gullies" and "ridges" at high enough grafting density.[16] The physical reason for the transformation is explained by the advantage of nonuniform vertical stretching of polymer chains at high grafting density.[16]

All mentioned above ways of orientation of nanodomains in the films are based on reaching thermodynamic equilibrium. However, in many cases, fast preparation of the films keeps the system away from the equilibrium. For example, the most common way of preparation, spin-coating, is based on the spreading of a droplet of polymer solution on the substrate under action of inertia force which is accompanied by fast solvent evaporation. The resulting nanodomain structure does not necessarily correspond to the equilibrium one and usually reveals many defects. In order to approach equilibrium, the film is subjected to annealing. Thermal annealing, i.e., heating up the film, leads to an increased mobility of the macromolecules and improvement of the ordering. Further slow cooling to the initial temperature brings (or approaches) the system to the equilibrium state. Improvement of the long-range order[1] of the nanodomains can also be achieved by applying an electric field to copolymers differing in the dielectric constant of the blocks, such that the domains orient in the direction of the field.[17,18] However, enforced domain orientation does not necessarily lead to equilibrium.

Another way to equilibrate the system is so-called solvent vapor annealing. The sample is exposed to a solvent vapor, some fraction of which is absorbed by the film. The absorbed molecules play the role of a lubricant making the macromolecules more mobile. That is why the equilibrium structure in the swollen film can be reached more easily than in the dry film. After slow drying, the film can "improve" its initial ordering. Applying the swelling−drying procedure in a cyclic manner, one can equilibrate the system.

The structural changes in dry thin films during thermal annealing are quite predictable and comprise either the order-to-disorder transition[19,20] (in case of a broad temperature variation) or a change of the segregation regime, i.e., weak or strong segregation. In contrast, absorption of vapor molecules during solvent vapor annealing makes the system three-component (two blocks and condensed solvent), where structural changes are strongly influenced by the interaction of the two polymer blocks with the solvent, the distribution of solvent in the film, etc. In other words, the swollen film is a more complicated system which is less easily understood than the dry films. Thus, the main objective of the present paper is to study the swelling of lamellae-forming diblock copolymer films using dissipative particle dynamics (DPD) computer simulations and mean-field calculations.

Experimental studies of structural changes during solvent annealing are quite extensive.[21−30] In particular, it has been detected recently using grazing-incidence small-angle X-ray scattering (GISAXS) that solvent uptake by thin films having initially the parallel lamellar orientation results in formation of additional lamellae which, eventually, have a smaller thickness than the dry ones.[27,30] In the present paper, we quantify this effect. Computer simulations results will be compared with experimental data. We also study the swelling of films with the perpendicular lamellar orientation. The effect of concentration of the solvent at interfaces and its penetration even through solvophobic films will be discussed.

MODEL AND SIMULATION METHOD

Our modeling is based on the dissipative particle dynamics (DPD) simulation technique.[31,32] The simulations are performed in a tetragonal box of a constant volume $V = L_x \cdot L_y \cdot L_z = 40 \cdot 40 \cdot 100$ with periodic boundary conditions in the x and y directions (i.e., in the film plane). All quantities are measured in units of the mass of the polymer bead, m_0, thermal energy, k_BT, and the cutoff radius of the interaction potential, r_c. Thus, for simplicity, we fix them as $m_0 = k_BT = r_c = 1$. We set the total number density in the system as $\rho = N/V = 3$, so that the total number of the particles in the box is $N = 3 \cdot 40^2 \cdot 100$. There are four different types of particles in the system: solvent particles (denoted by S), A- and B-beads forming diblock copolymers, and the particles forming the walls at $z = 0$ (bottom) and $z = L_z$ (top) (denoted by W). The W-particles are arranged to form smooth, dense walls which prevent escape of all other particles from the system. We model the walls by assuming that each of them consists of two identical solid layers of immobile (frozen) DPD particles arranged in a regular array and stuck on the top ($z = 0$) or bottom ($z = L_z$) boundaries. To avoid the penetration of polymer and solvent particles into the wall, the nearest W-particles inside each layer are separated by a distance of $\rho\sigma^{-1/3}$, and the distance between the layers within each wall is $0.8\rho\sigma^{-1/3}$. In addition, two contacting layers are shifted relative to each other at a distance of $0.5\rho\sigma^{-1/3}$ along the x- and y-axis. The forces acting between any pair of DPD particles are taken to be the same nature for both mobile and frozen particles. In the course of the simulation, we do not update the positions of the W-particles, implicitly assuming that they have an infinite mass, but in the calculation of the dissipative forces we attribute to those particles a velocity randomly selected from the Maxwell−Boltzmann distribution, corresponding to the target temperature, to avoid the development of temperature gradients near the walls. By setting the boundaries of the system in this way, we eliminate the possible role of the wall-slippage effect.

The volume above the film is filled with single-site solvent particles (the initial structure before annealing of the system). The polymer volume fraction in the box corresponds to 40%. We fix the number of the beads in each block at 10, so the total number of the beads in the polymer chain is $n = 20$ (we consider only symmetric copolymers). The force keeping the beads in the chains is described by Hooke's law, $F_{ij}^s = -C_s(r_{ij} - r_{eq})$, with the spring constant $C_s = 3$ and the equilibrium distance between the attracting particles $r_{eq} = 1$. The starting structures of the system before annealing correspond to complete separation of the polymer and solvent. Therefore, the dry film swells during annealing; i.e., it takes up solvent. Furthermore, to prove convergency to the equilibrium structure, each time we prepare two different initial structures of the dry film (spatially homogeneous and lamellar) and let them relax during the swelling process. We restrict ourselves to

dx.doi.org/10.1021/ma400810u | Macromolecules 2013, 46, 5786−5795

the analysis of a nonselective solvent; i.e., interactions of the solvent molecules with A and B species are quantified by equal parameters. The DPD method is based on the solution of the Newtonian equations of motion for all particles in the system. Each particle is subjected to the action of three different pairwise-additive forces: conservative, dissipative, and random. The conservative force is characterized by soft repulsion between nonbonded particles via the interaction parameters a_{ij}. The complete set of parameters is presented in Tables 1 and 2.

Table 1. DPD Interaction Parameters Used in Simulations of Parallel Lamellae[a]

a_{ij}	A	B	S	W_{bottom}	W_{top}
A	25	40	a_{AS}	25	25
B	40	25	a_{BS}	50	25
S	a_{AS}	a_{BS}	25	50	25
W_{bottom}	25	50	50	25	25
W_{top}	25	25	25	25	25

[a]The interaction parameters are represented in units of k_BT/r_c. The strength of AS and BS repulsions is varied (see text).

Table 2. DPD Interaction Parameters Used in Simulations of Perpendicular Lamellae

a_{ij}	A	B	S	W_{bottom}	W_{top}
A	25	40	a_{AS}	25	25
B	40	25	a_{BS}	25	25
S	a_{AS}	a_{BS}	25	50	25
W_{bottom}	25	25	50	25	25
W_{top}	25	25	25	25	25

The inequality $a_{AA} = a_{BB} < a_{AB}$ means that A and B beads are incompatible even in the presence of the solvent. In general, one can estimate the Flory–Huggins parameters according to the formula:[33] $\chi_{ij} = (0.286 \pm 0.002)(a_{ij} - a_{ii})$ at $\rho = 3$. For a nonselective solvent $a_{AS} = a_{BS}$, and its quality is determined by the absolute value of a_{AS}. In our calculations, this parameter varies in the interval between 29 and 40. The latter value corresponds to very poor solvent in which the film does not swell (dry state). On the contrary, the swollen film starts to dissolve at about $a_{AS} = 29$.

The dissipative and random forces are specified by the friction coefficients, g_{ij}, and noise amplitudes, σ_{ij}, respectively, and play the role of the heat sink. They satisfy the fluctuation–dissipation theorem, $\sigma_{ij}^2 = 2g_{ij}$, and in our simulations σ_{ij} is set to be 3. The equations of motion are integrated using a self-consistent leapfrog scheme[34] with a time step $\Delta t = 0.05$. The number of the time steps for equilibration of the system is 10^6.

The annealing of the system is carried out in two ways. In the case of initial spatially disordered state of the dry film, we slowly change the DPD force parameters during the equilibration run, until they reach the values of interest $a_{\beta\alpha}$ (cf. Tables 1 and 2), and an ordered state is achieved. This simulation-annealing procedure follows the usual linear schedule, $a_{\beta\alpha}(s) = a_{\alpha\alpha} + (a_{\beta\alpha} - a_{\alpha\alpha})s/n_s$, where the initial values $a_{\alpha\alpha}$ are set to 25, $a_{\beta\alpha}(s)$ are the force parameters at time step s, and n_s is the number of time steps (10^6). This strategy is analogous to slow cooling a real block copolymer films across the disorder-to-order transition. In the case of initial lamellar structure of the dry film, we "switch on" the necessary values of $a_{\beta\alpha}$ and let the system relax during the swelling process.

PARALLEL ORIENTATION OF LAMELLAE

As we mentioned above, the orientation of nanodomains in block copolymer thin films is primarily controlled by interactions with confining surfaces. The most widespread, so-called free-surface films are formed on a solid substrate and have a "free" upper surface in contact with air (vapor). For such

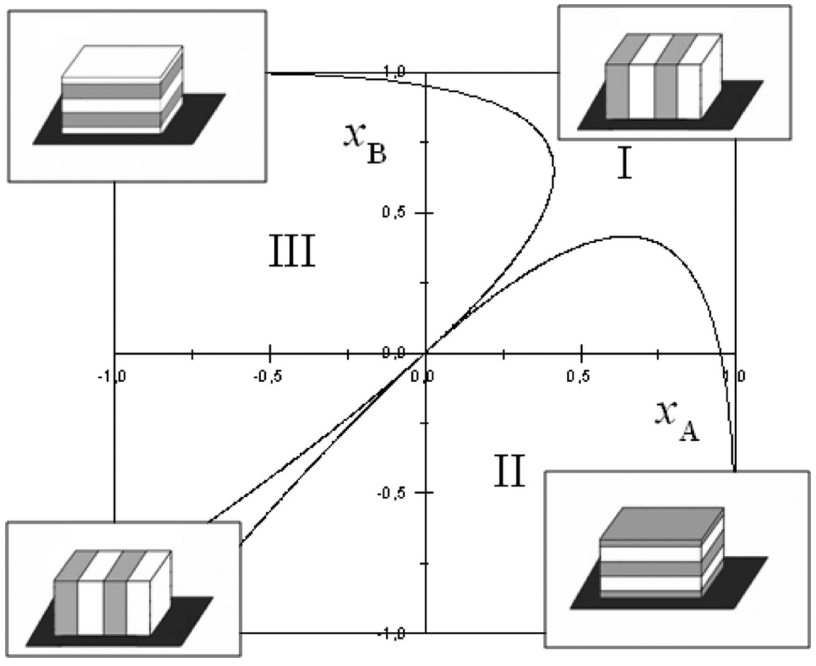

Figure 1. Diagram of lamellar orientations in dry free-surface films of symmetric AB diblock copolymers.[6] Dimensionless variables $x_{A,B}$ are the ratios of the spreading coefficients $S_{A,B}$ to the reduced thickness of the film (see text), $n + 1$, and to the interdomain surface tension coefficient γ_{AB}, $x_{A,B} = S_{A,B}/(n + 1)\gamma_{AB}$. Roman numerals depict regions of thermodynamic stability of perpendicular lamellae (I), symmetric structure of parallel lamellae with A boundary layers (II), and symmetric structure of parallel lamellae with B boundary layers (III).

dx.doi.org/10.1021/ma400810u | Macromolecules 2013, 46, 5786–5795

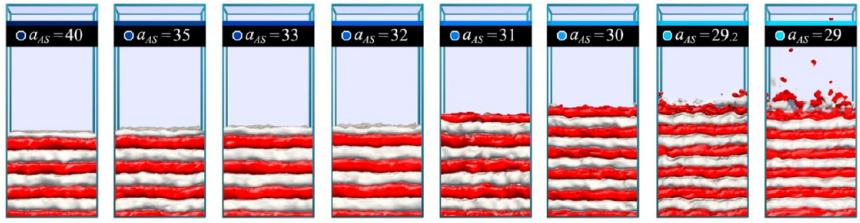

Figure 2. Snapshots of the film with parallel lamellae at different degrees of swelling: dry film (a_{AS} = 40), affine swelling (a_{AS} = 40−32), swelling with increasing number of lamellae (a_{AS} = 31−29.2), and dissolution of the film (a_{AS} = 29).

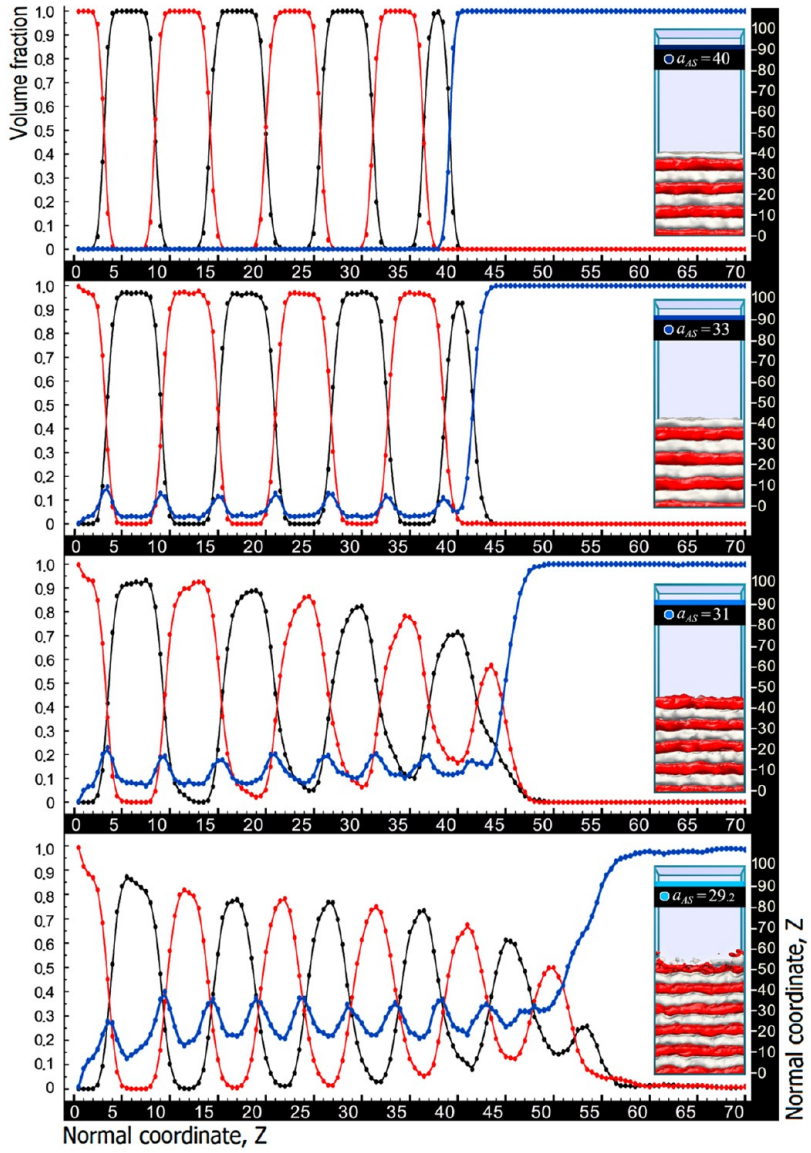

Figure 3. Volume fractions of monomer A (red), monomer B (black), and solvent (blue) inside the film with parallel lamellar orientation as functions of the normal coordinate z. The snapshots correspond to the profiles. The numbers at the top of the box depict the corresponding values of the parameter a_{AS}.

films formed by symmetric diblock copolymers, the lamellar orientation depends on the spreading coefficients S_A and S_B of A and B blocks.[6] The spreading coefficient $S_A = \gamma_{sa} - \gamma_{Aa} - \gamma_{As}$ (an analogous for S_B) is a combination of the substrate−air (sa), A block−air (Aa), and A block−substrate (As) surface tension coefficients. If $S_A > 0$, the A block spreads on the substrate; i.e., the contacts of the A block with the substrate are favorable. In the opposite case, $S_A < 0$, the A block only partially wets the substrate, and its contact with the substrate is less favorable than in the spreading regime. The diagram of lamellar orientations in the free-surface film of the symmetric diblock copolymer can be presented in dimensionless variables $x_A = S_A/(n + 1)\gamma_{AB}$ and $x_B = S_B/(n + 1)\gamma_{AB}$ (Figure 1).[6] Here n is the total number of A and B layers in the case of the parallel lamellar orientation; each layer of a thickness equal to the half-period, $D_{||}/2$, which is related to the film thickness H via $n + 1$

dx.doi.org/10.1021/ma400810u | Macromolecules 2013, 46, 5786−5795

= $2H/D_{||}$; γ_{AB} is the interdomain surface tension coefficient. The most important conclusions from the diagram can be summarized as follows. The perpendicular lamellae are stable if the interactions of both A and B blocks with the substrate (spreading coefficients) are similar (neutral substrate[7]). Furthermore, reliable stability of the perpendicular orientation is achievable for thinner films in the regime of spreading ($x_A \approx x_B \sim 1$, the region far from the boundaries, Figure 1). If the interactions of the blocks with the substrate are dissimilar, the parallel structure is more stable. For example, the spreading (favorable contacts) of A blocks on the substrate, $x_A > 0$, and partial dewetting (unfavorable contacts) of B blocks from the substrate ($x_B < 0$) induce the parallel orientation of the lamellae with boundary A layers (symmetric structure).

To induce the parallel lamellar orientation in computer simulations, we use different interaction parameters presented in Table 1. The inequality $a_{AW} < a_{BW}$ for the polymer beads interacting with the bottom wall means that the repulsion of the B blocks from the wall is higher; i.e., contacts of A blocks with the wall (substrate) are more favorable.

After annealing of the polymer film at $a_{AS} = 40$, the parallel lamellar structure is formed (Figure 2). In this structure, the bottom ("red") half-layer is formed by A blocks ($a_{AW} < a_{BW}$). After six alternating full layers of B and A types, the upper half-layer of the type B is complete (so-called antisymmetric wetting). The solvent does not penetrate into the film at $a_{AS} = 40$ (dry film) which is demonstrated by the blue curve in Figure 3. The sum of the volume fractions of A and B blocks inside the corresponding domains is equal to unity, and the shape of the polymer density profile allows us to assume the strong segregation regime in the dry film (Figure 3). The decrease of the parameter a_{AS} leads to the swelling of the film. One can distinguish two regimes of lamellar swelling. (i) Affine swelling of the film (swelling of individual lamella with their number in the film being fixed) is observed at the decrease of a_{AS} down to 32 (Figures 2−4). (ii) Below this value, a reduction of the

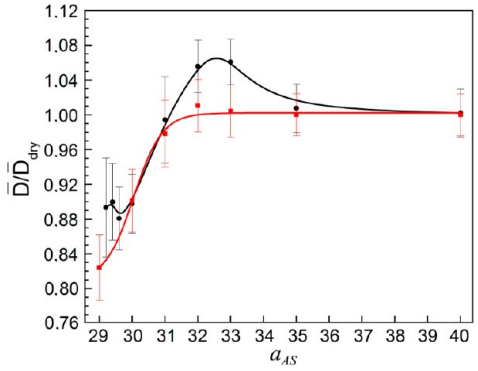

Figure 4. Ratio of the average lamellar thickness of the swollen film, $\bar{D}$, to the thickness of the lamella in the dry film, $\bar{D}_{dry}$ (reduced thickness), as a function of the solvent quality: parallel (black) and perpendicular (red) lamellae. The averaging is carried out on the basis of full layers of A and B blocks.

lamellar thickness and an increase of the number of lamellae occur. The latter effect is due to the weakening of the incompatibility between A and B monomer units in the presence of the solvent. It makes the blocks less stretched. On the other hand, the AB interfacial area per molecule increases; i.e., the chains become more coiled. Therefore, the number of the lamellae grows and their thickness decreases. The initial swelling of the lamellae (Figure 4) is related to a finite size effect in z-direction (finite number of the lamellae). Structural changes in the film correspond to the lower free energy if the upper layer is complete. Any terraces formation in the upper layer at the length scale of the simulation box (nanoscale) costs extra surface energy, especially in the case of poor solvent. Therefore, if the fraction of the absorbed solvent is small and the increasing area of AB interfaces is insufficient to form an additional complete AB layer, the alternative process of swelling of the fixed number of lamellae is the only way to provide the film swelling. It is clear that the higher the number of lamellae in the dry film, the less pronounced the effect of the affine swelling. It disappears in the limit of infinite number of lamellae (bulk limit).

All above-mentioned reasoning is supported by the dependence of the thickness of an individual layer on the solvent quality (parameter a_{AS}) (Figure 5). The upper and bottom

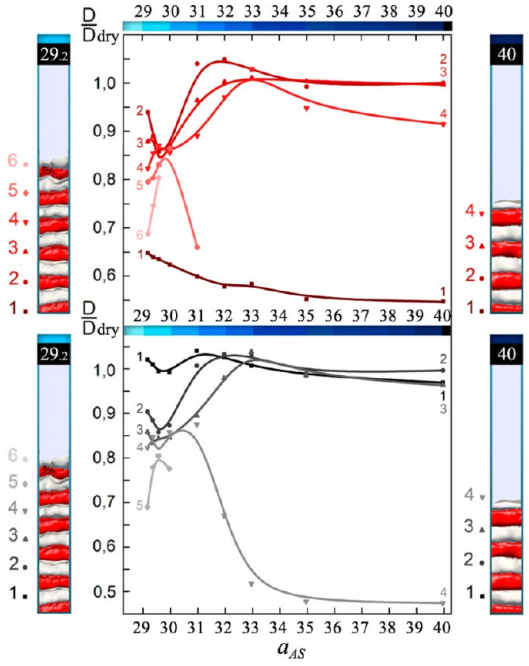

Figure 5. Dependence of the reduced thickness of A (upper plot) and B (bottom plot) layers on the solvent quality. Left and right snapshots depict the swollen and the dry film, respectively. 1, 2, 3, ... number the corresponding layers.

plots correspond to A ("red") and B ("gray") layers, respectively (1, 2, ... number the corresponding layers, A half-layer being the first). It is seen that there are four A and four B layers in the interval between $a_{AS} = 32$ and 40. Each of them gets swollen with the decrease of a_{AS}, especially the upper B half-layer (no. 4). However, it transforms into the full layer and additional A half-layer (no. 5) appears atop the film at $a_{AS} = 31$ (Figure 5). Then, the A layer becomes full and B half-layer (no. 5) completes the film at $a_{AS} = 30$, etc.

The decrease of the lamellar thickness in the swollen film can easily be demonstrated using the strong segregation approach[30,35] which is well applicable for a low degree of swelling and long molecules ($\phi\chi_{AB}n \gg 1$). Within this approach, the free energy of the system per chain is a sum of the elastic and the interfacial contributions:[30]

dx.doi.org/10.1021/ma400810u | Macromolecules 2013, 46, 5786−5795

$$\frac{F_{lam}}{k_BT} = C\frac{D_{lam}^{\ 2}}{4a^2n} + \frac{2\gamma(\phi)a^3n}{k_BTD_{lam}\phi} \quad (1)$$

Here, effects of the substrate and the free surface on the domain structure are neglected which can be justified for thick enough films.[6] The first term in eq 1 is the elastic contribution, where a and n are the length of the segment of the chain, which is assumed to be the same for both blocks, and the total number of the segments in the chain (each block consists of $n/2$ segments), respectively. The period of the lamellar structure D_{lam} includes two full layers of A and B types. The numerical factor C depends on the model used. If an inhomogeneous distribution of the free ends is taken into account,[36] $C = \pi^2/8$. If the free ends are equidistant with respect to the AB interface, $C = 3/2$. The second term in eq 1 is the energy of AB interfaces per chain, $2\gamma(\phi)A/k_BTQ$, where A is the area of the interface, Q is the aggregation number (the number of chains per lamella), and k_BT is the thermal energy. These parameters are connected through the space filling condition. Assuming that the solvent is nonselective for both blocks, i.e., that both layers of the lamella have equal swelling coefficients and that the solvent is homogeneously distributed throughout the film, one can write $D_{lam}A\phi = QNa^3$. Homogeneous solvent distribution can be justified only for the case of very long molecules and a relatively low value of χ_{AB} (comparable with χ_{AS}), which, however, still provides the strong segregation regime ($\phi\chi_{AB}n \gg 1$). The surface tension coefficient $\gamma(\phi)$ of the AB interface depends on the polymer concentration. The mean-field calculations (theta and poor solvent) in the limit of a homogeneous solvent distribution and the scaling estimations (good solvent) give the same dependence on ϕ (see ref 30):

$$\bar{\gamma} = \gamma(\phi)a^2/k_BT = \sqrt{\chi_{AB}/6}\,\phi^{3/2} \quad (2)$$

This result reflects the fact that the lower the polymer volume fraction, the weaker the AB interactions per unit area. Thus, minimization of eq 1 with respect to the parameter D_{lam} leads to

$$D_{lam} = \left(\frac{8\chi_{AB}}{3C^2}\right)^{1/6}\phi^{1/6}aN^{2/3}$$

$$D_{lam}/D_{lam}^{dry} = \phi^{1/6} \quad (3)$$

which indicates the decrease of the lamellar thickness at the film swelling.

In real and computer experiments, the polymer chains have a finite length. Furthermore, the incompatibility of A and B monomer units in regime ii of the swelling is stronger than the one of the monomer units with the solvent ($a_{AB} = 40$ and $a_{AS} = 33-29$). Thus, the approximation of homogeneous distribution of the solvent is violated in this regime. The solvent volume fraction profile reveals local maxima at the AB interfaces (Figure 3). They appear to shield unfavorable contacts between A and B monomer units, thus decreasing the energetic contribution to the total free energy. Therefore, the spreading of the solvent within the film proceeds mainly through the interfaces. Keeping in mind that the initial orientations of domains in block copolymer films can be different (parallel, perpendicular, mixed, etc.), one can expect that kinetics of the swelling is also different. Accumulation of the solvent at the lamellar interfaces in bulk diblock copolymer solutions was also predicted theoretically[37] and was demonstrated recently in computer simulations.[38]

Despite the complicated swelling behavior of the individual layers, the overall swelling of the film is one-dimensional (in z-direction). It is described by the simple expression $H/H_{dry} = 1/\phi$, where H and H_{dry} are the thicknesses of the swollen and dry films, respectively. In computer simulations, this result reflects the fact of the periodic boundary conditions in the xy-plane, i.e., of the infinite (in the thermodynamic limit) area of the film. Very thin films in the regime of spreading (the spreading coefficients for A and/or B blocks are positive) can change their area during swelling.[6] However, the swelling in the z-direction (nano- and micrometers) is a much faster process than the spreading in xy-plane (macroscopic dimensions). Thus, the approximation of fixed film area is good enough. The reduced film thickness monotonously increases with improving solvent quality (decreasing parameter a_{AS}) due to absorption of the solvent molecules (Figure 6).

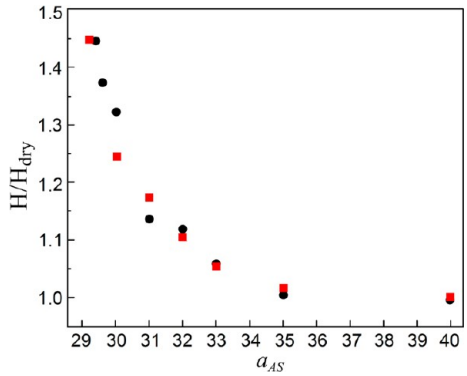

Figure 6. Reduced film thickness as a function of the solvent quality: parallel (black circles) and perpendicular (red squares) lamellae.

The kinetics of the film swelling and evolution in time of the lamellar thickness is presented in Figure 7. The lamellae affinely swell during the initial time interval (for example, up to 3×10^5 time steps at $a_{AS} = 31$). This stage is just a manifestation of the fact that diffusion of the low-molecular-weight solvent molecules into the film is a faster process than the shrinkage (decrease of the stretching) of the polymer chains in the lamellae due to the shielding of the repulsive interaction between different blocks. Only after 3×10^5 time steps, the chains start to shrink. This leads first to the decrease of the lamellar thickness at a fixed number of chains per lamella (fixed aggregation number). Shrinkage in one direction results in an extension in perpendicular ones; thus, the lamellar area increases. On the other hand, the total area of the film is constant, and the increase of the area of parallel lamellae has to be accompanied by their undulations to fulfill the space filling condition. Subsequently, the lamellae break apart with formation of additional lamellae, each having a smaller thickness and aggregation number than the dry ones (Figure 7). Similar behavior was detected experimentally using GISAXS.[27]

PERPENDICULAR ORIENTATION OF LAMELLAE

As demonstrated in Figure 1, the perpendicular lamellar orientation is stable if the interactions of both blocks with the substrate are similar (similar spreading coefficients). To realize the effect of the "neutral" substrate in computer simulations, the interaction parameters of A and B blocks with the bottom substrate are chosen to be equal (Table 2). All

dx.doi.org/10.1021/ma400810u | Macromolecules 2013, 46, 5786−5795

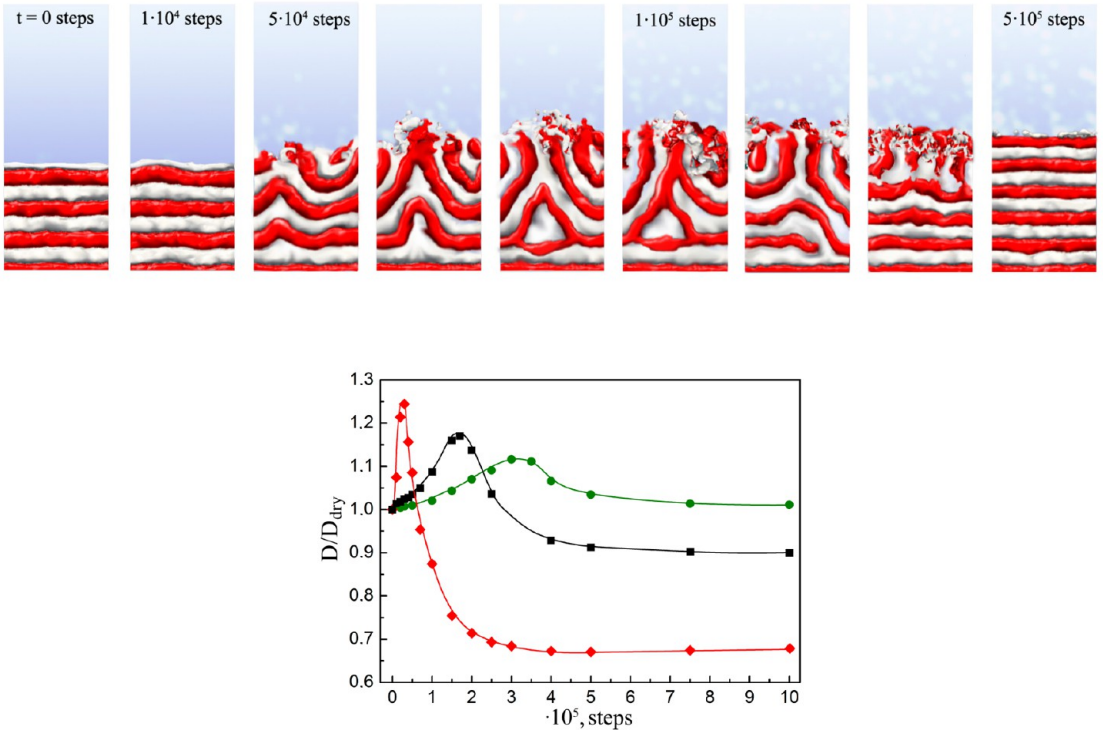

Figure 7. Time evolution of the parallel lamellar structure during swelling at a_{AS} = 29 (upper snapshots). Reduced lamellar thickness (average value) as a function of time steps for different solvent qualities: a_{AS} = 29 (red diamonds), 30 (black squares), and 31 (green circles).

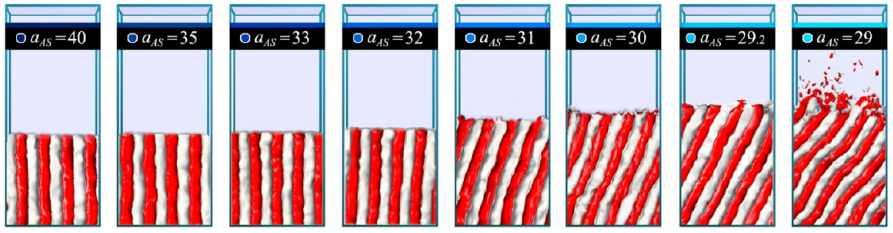

Figure 8. Snapshots of perpendicular lamellae which tilt during the film swelling: dry (a_{AS} = 40) and swollen film (a_{AS} = 35–29). The film dissolution starts at a_{AS} slightly lower than 29.

other parameters (composition of the molecules, box dimensions, etc.) are the same as in the above-described simulations of the parallel lamellae. We consider two initial structures of the film: perpendicular lamellae and spatially disordered ones. In both cases, a dry film with perpendicular lamellae is formed after annealing at a_{AB} = 40 and a_{AS} = 40 (Figure 8). The average thickness of the dry perpendicular lamellae is equal to the one of the parallel lamellae (Figure 4). However, the swelling of the film with perpendicular lamellae proceeds differently. First of all, the regime of the lamella thickening is absent for the perpendicular lamellae; i.e., D/D_{dry} monotonously decays with the decrease of a_{AS} (Figure 4) (a weak nonmonotonicity is within the accuracy of the calculations). Such behavior is to be expected because the swelling of the film is not accompanied by the formation of extra parallel complete lamella. The absorbed solvent makes the perpendicular lamellae thinner (e.g., along the *x*-axis). This leads to an increase of the lamellar area in the *y*- and *z*-directions, if the number of lamellae remains the same. Keeping in mind the fixed area of the film, the increase of the lamellar dimension in the *y*-direction results in a zigzag bending of the lamellae. In order to fulfill the space filling condition in the *x*-direction, the lamellae must tilt (Figure 8), which is confirmed by calculation of the tilt angle θ (deviation of the lamella plane from the substrate normal), $\cos\theta \approx D/D_{dry}$. An obvious question is whether the tilted lamellae are in equilibrium or not. In other words, what is more favorable for the lamellae: to tilt or to increase their number to remain perpendicular? In order to answer this question, we did the following "annealing". First, to avoid the finite size effect, the *xy*-dimensions of the box were varied in small steps ("tuned"): 41 × 41, 42 × 42, 43 × 43, etc. Also, a much larger box was considered (80 × 80 × 60). Furthermore, to accelerate reorganization of the lamellar structure, the film was dissolved at a_{AS} = 28 and then condensed again at different values of a_{AS} (higher than 29). It turns out that swollen perpendicular lamellae are formed if their thickness is commensurable with the lateral box size (Figure 9). This means that the perpendicular orientation of the lamellae in the swollen state is more favorable and corresponds to the absolute minimum of the free energy (compared to the tilted lamellae). However, if the vapor uptake does not lead to the order-to-disorder transition and the restoring of the lamellar structure in real experiments (an analogue of the film dissolution and condensation in computer experiment), the

dx.doi.org/10.1021/ma400810u | *Macromolecules* 2013, 46, 5786–5795

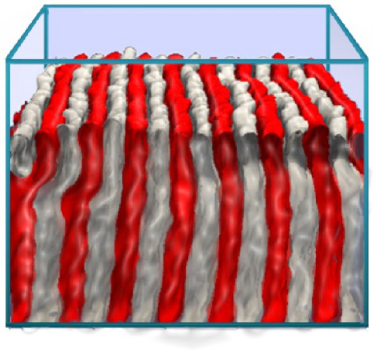

Figure 9. Snapshot of swollen perpendicular lamellae obtained in a bigger box (80 × 80 × 60) at a_{AS} = 31. The number of the molecules in this box is chosen such that the same thickness of the dry film as in the smaller box is obtained.

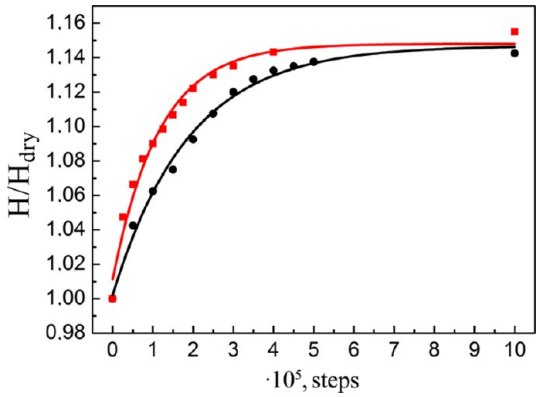

Figure 10. Reduced film thickness as a function of time steps at a_{AS} = 31: parallel (black circles) and perpendicular (red squares) lamellar orientations.

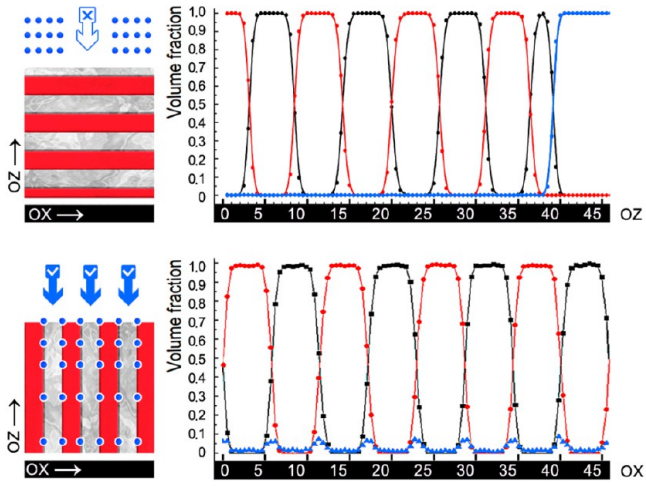

Figure 11. Solvent (blue dots) distribution in solvophobic films (a_{AS} = a_{BS} = 40) composed of block copolymers with strongly incompatible blocks (a_{AB} = 45). Polymer A (red), polymer B (black), and solvent (blue) volume fractions in the film with the parallel (upper plot) and the perpendicular (bottom plot) lamellar orientation as a function of the normal (with respect to the lamellae) coordinate.

lamellar splitting during the swelling and an approach of the equilibrium is a hardly realizable process which requires large-scale in-plane mass transport. Instead, the lamellar thinning to the true equilibrium value (as for the equilibrium perpendicular lamellae) and tilting is a much faster process. A nonsignificant increase of the free energy per chain of the tilted lamellae is caused by an entropic penalty of the chains in the vicinity of the substrate and the free surface which becomes less important with increasing film thickness. Therefore, one can expect that in a real experiment the tilting of the perpendicular lamellae during the film swelling is the most probable scenario.

The solvent distribution in the perpendicular and tilted lamellae is also inhomogeneous: a higher fraction is localized at the AB interfaces. The overall degree of swelling of the film with perpendicular and tilted lamellae is nearly the same as in the case of parallel lamellae (Figure 6). This effect is a consequence of (i) the nonselective solvent (the domains of both sorts behave similarly) and of the fact that (ii) the interfacial area per molecule for parallel and perpendicular lamellae is nearly the same. Otherwise, a redistribution of the solvent between domains and interfaces would lead to different degrees of swelling. However, due to the different orientations of the domains with respect to the free surface, one can expect different swelling rates, especially in the case of a selective solvent. The films with perpendicular (tilted) lamellae swell faster because a higher amount of solvent penetrates through the AB interfaces, which are exposed to the free surface. On the contrary, the parallel lamellae create a kind of "barriers" slowing down the swelling. In the case of a_{AS} = 31, the swelling of the film with perpendicular lamellae is approximately 2 times faster than the swelling of the film with the parallel lamellae (Figure 10). For example, a degree of swelling of 1.1 is achieved after 10^5 and 2 × 10^5 time steps for perpendicular and parallel lamellae, respectively. Furthermore, one can expect that diblock copolymer films based on two solvophobic blocks can be penetrable for a solvent, if the lamellae have the perpendicular (tilted) orientation. In this case, despite an incompatibility with both the A and the B blocks, the solvent can be localized at the AB interfaces to reduce the energy of unfavorable AB contacts, if this energy is higher than the energy of polymer−solvent contacts. A characteristic distribution of the solvent in solvophobic film is presented in Figure 11 at a_{AB} = 45 and a_{AS} = 40. Therefore, such films with perpendicular domain orientation can be used as membranes with nanochannels.

EXPERIMENTAL STUDIES

The computer simulations of the swelling of parallel lamellae are compared with experimental data. A poly(styrene-*b*-butadiene), PS-*b*-PB, diblock copolymer having a molar mass of 22.1 kg/mol, a PB volume fraction of 0.49 ± 0.01, and a bulk lamellar thickness D^{bulk} = 18.9 nm was studied.[39] A thin film was spin-cast from toluene solution on Si wafers terminated with a native SiO_x layer and was annealed in vacuum at 150 °C for 12 h. The film thickness in the as-prepared state was 100 nm, as determined with a spectroscopic reflectometer (Filmetrics 20X, San Diego, CA). The film thus consisted initially of 5.7 stacked lamellae on average. GISAXS experiments were performed at CHESS beamline D1 with the vapor cell mounted on a goniometer and a CCD camera as an area detector. The angle of incidence, α_i, was chosen to be 0.24°. The critical angles of total external reflection from PS-*b*-PB and from SiO_x are 0.15° and 0.22° at the X-ray wavelength chosen, respectively; i.e., scattering from the whole film is observed.

Toluene, a good and close to nonselective solvent,[40] was injected into a reservoir in the sample cell through a long Teflon capillary, and GISAXS images were taken subsequently every 10 s with an exposure time of 3 s while the film was immersed in saturated vapor. All measurements were carried out at room temperature. The peak positions were analyzed by fitting Lorentz functions to the peaks in the intensity profiles along q_z, i.e., along the film normal.

dx.doi.org/10.1021/ma400810u | *Macromolecules* 2013, 46, 5786−5795

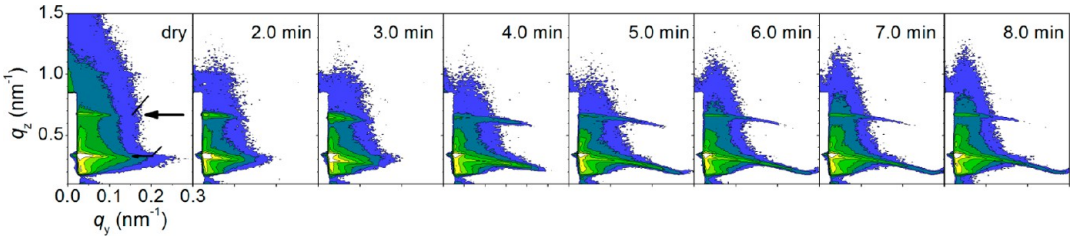

Figure 12. Two-dimensional GISAXS maps before and during vapor treatment with saturated toluene vapor. The horizontal arrow marks the diffuse tail of the first-order DBS. The time intervals after toluene injection are indicated.[27] The logarithmic intensity scale runs from 8 (blue) to 2000 (yellow).

Before vapor treatment, the lamellae in the film were aligned parallel to the film surface, as revealed by the presence of diffuse Bragg sheets (DBS) appearing along the film normal, q_z, and extending along q_y (Figure 12, first image). The DBS's are associated with the correlated roughness of lamellae, having their interfaces parallel to the substrate surface.[42,43] The lamellar thickness in the thin film geometry, D, was determined within the distorted-wave Born approximation (eq 26 in ref 41); i.e., from the q_z positions of the DBS's,[41] D was found to be similar to D^{bulk}.

After solvent injection, a constant vapor pressure in the cell was rapidly established, and the vapor entered the film, as reflected by the immediate increase in H (not shown). 2D GISAXS images of the film taken after the injection of toluene into the cell are shown in Figure 12. During the first 3.5 min of solvent vapor exposure, the DBS's moved downward; then, they moved again toward larger q_z values. The lamellar thickness thus first increases during approximately 3.5 min and then decreases again (Figure 13). This behavior is well reproduced

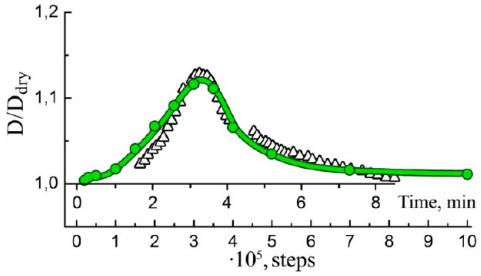

Figure 13. Experimental values of the reduced lamellar thickness D/D_{dry} as a function of swelling time (black triangles).[27] Filled green circles and the fitting line correspond to the computer simulations of the swelling of a parallel film at a_{AS} = 31.

in our computer simulations. The filled green circles and the fitting line in Figure 13 correspond to computer simulations obtained during relaxation of the parallel lamellar structure to the equilibrium value at a_{AS} = 31. The initial swelling of the lamellae is caused by fast uptake of the vapor molecules. The subsequent decrease of D after 3.5 min demonstrates the shrinkage of the diblock copolymer domains because of the shielding of the repulsion between different blocks.

CONCLUSION

In conclusion, we have demonstrated using DPD simulations that the lamellar orientation in thin films of symmetric diblock copolymer depends on the interactions of the blocks with the substrate (bottom wall). Parallel lamellae are stable if one of the blocks has an affinity to the substrate. Equal interaction parameters for both blocks result in the perpendicular lamellar orientation (neutral substrate). The swelling of the films in a low-molecular-weight solvent was studied. The general effect of the absorbed solvent is the shielding of the effective repulsion between different blocks leading to copolymer decreased stretching and lamellar thinning. However, in the case of parallel lamellae, this effect can be observed only at a high degree of swelling of the film when a complete additional lamella (or an integer multiple) can be formed. Otherwise, the film swelling can proceeds only via swelling of the individual lamellae. Thus, the thickness of the parallel lamellae reveals nonmonotonous behavior as a function of the degree of swelling. The perpendicular lamellae do not swell; i.e., their thickness does not increase. Their thinning leads to the formation of a higher number of the perpendicular lamellae. However, such an equilibrium state is hardly achievable experimentally because it requires large-scale mass transport. A tilting of the fixed number of the lamellae during swelling is a much faster process. One can expect that the metastable state of the tilted lamellae is the most probable realization in real experiments. We have demonstrated that the solvent condensed in the film has an inhomogeneous distribution; it accumulates at the AB interfaces. This effect is also a consequence of the shielding of unfavorable contacts between the blocks: the higher the incompatibility, the higher the difference between the solvent concentrations at the interface and inside the domains. Such a tendency of the solvent to be localized at the interfaces results in different penetration rates of the solvent through the films with different orientations of the domains. Furthermore, we have demonstrated that even films from solvophobic blocks can be penetrable for the solvent if the lamellae have the perpendicular orientation.

AUTHOR INFORMATION

Corresponding Author

*E-mail: igor@polly.phys.msu.ru (I.I.P.).

Notes

The authors declare no competing financial interest.

ACKNOWLEDGMENTS

The financial support of the Russian Foundation for Basic Research, the Ministry of Education and Science (Russian Federation), the German Federal Ministry of Education, and the German Research Foundation (Pa771/7-1) is gratefully acknowledged. The simulations were performed on multi-teraflop supercomputers Lomonosov and Chebyshev at Moscow State University. This work is partially based upon research conducted at beamline D1 at the Cornell High Energy Synchrotron Source (CHESS). CHESS is funded by the National Science Foundation and the National Institutes of Health/National Institute of General Medical Sciences under NSF Award DMR-0936384.

REFERENCES

(1) Thurn-Albrecht, T.; Schotter, J.; Kästle, G. A.; Emley, N.; Shibauchi, T.; Krusin-Elbaum, L.; Guarini, K.; Black, C. T.; Tuominen, M. T.; Russell, T. P. *Science* **2000**, *290*, 2126−2129.
(2) Topham, P. D.; Parnell, A. J.; Hiorns, R. C. *J. Polym. Sci., Part B* **2011**, *49*, 1131−1156.
(3) Urbas, A.; Fink, Y.; Thomas, E. L. *Macromolecules* **1999**, *32*, 4748−4750.
(4) Jung, Y. S.; Jung, W.; Tuller, H. L.; Ross, C. A. *Nano Lett.* **2008**, *8*, 3776−3780.
(5) Turner, M. S.; Johner, A.; Joanny, J.-F. *J. Phys. I* **1995**, *5*, 917−932.
(6) Potemkin, I. I. *Macromolecules* **2004**, *37*, 3505−3509.
(7) Ryu, D. Y.; Wang, J.-Y.; Lavery, K. A.; Drockenmuller, E.; Satija, S. K.; Hawker, C. J.; Russell, T. P. *Macromolecules* **2007**, *40*, 4296−4300.
(8) Busch, P.; Posselt, D.; Smilgies, D.-M.; Rheinländer, B.; Kremer, F.; Papadakis, C. M. *Macromolecules* **2003**, *36*, 8717−8727.
(9) Potemkin, I. I.; Busch, P.; Smilgies, D.-M.; Posselt, D.; Papadakis, C. M. *Macromol. Rapid Commun.* **2007**, *28*, 579−584.
(10) Kim, S. O.; Solak, H. H.; Stoykovich, M. P.; Ferrier, N. J.; de Pablo, J. J.; Nealey, P. F. *Nature* **2003**, *424*, 411−414.
(11) Stoykovich, M. P.; Muller, M.; Kim, S. O.; Solak, H. H.; Edwards, E. W.; de Pablo, J. J.; Nealey, P. F. *Science* **2005**, *308*, 1442−1446.
(12) Kriksin, Yu. A.; Neratova, I. V.; Khalatur, P. G.; Khokhlov, A. R. *Chem. Phys. Lett.* **2010**, *492*, 103−108.
(13) Kriksin, Yu. A.; Khalatur, P. G.; Neratova, I. V.; Khokhlov, A. R.; Tsarkova, L. A. *J. Phys. Chem. C* **2011**, *115*, 25185−25200.
(14) Albrecht, K.; Mourran, A.; Zhu, X.; Markkula, T.; Groll, J.; Beginn, U.; de Jeu, W. H.; Möller, M. *Macromolecules* **2008**, *41*, 1728−1738.
(15) Potemkin, I. I.; Bodrova, A. S. *Macromolecules* **2009**, *42*, 2817−2825.
(16) Rudov, A. A.; Khalatur, P. G.; Potemkin, I. I. *Macromolecules* **2012**, *45*, 4870−4875.
(17) Morkved, T. L.; Lu, M.; Urbas, A. M.; Ehrichs, E. E.; Jaeger, H. M.; Mansky, P.; Russell, T. P. *Science* **1996**, *273*, 931−933.
(18) Olszowka, V.; Hund, M.; Kuntermann, V.; Scherdel, S.; Tsarkova, L.; Böker, A.; Krausch, G. *Soft Matter* **2006**, *2*, 1089−1094.
(19) Angerman, H. J.; Johner, A.; Semenov, A. N. *Macromolecules* **2006**, *39*, 6210−6220.
(20) Miao, B.; Yan, D.; Han, C. C.; Shi, A.-C. *J. Chem. Phys.* **2006**, *124*, 144902.
(21) Bosworth, J. K.; Paik, M. Y.; Ruiz, R.; Schwartz, E. L.; Huang, J. Q.; Ko, A. W.; Smilgies, D. M.; Black, C. T.; Ober, C. K. *ACS Nano* **2008**, *2*, 1396−1402.
(22) Park, S.; Lee, D. H.; Xu, J.; Kim, B.; Hong, S. W.; Jeong, U.; Xu, T.; Russell, T. P. *Science* **2009**, *323*, 1030−1033.
(23) Olszowka, V.; Hund, M.; Kuntermann, V.; Scherdel, S.; Tsarkova, L.; Böker, A. *ACS Nano* **2009**, *3*, 1091−1096.
(24) Kim, S. H.; Misner, M. J.; Xu, T.; Kimura, M.; Russell, T. P. *Adv. Mater.* **2004**, *16*, 226−231.
(25) Kim, T. H.; Hwang, J.; Hwang, W. S.; Huh, J.; Kim, H. C.; Kim, S. H.; Hong, J. M.; Thomas, E. L.; Park, C. *Adv. Mater.* **2008**, *20*, 522−527.
(26) Smilgies, D.-M.; Busch, P.; Papadakis, C. M.; Posselt, D. *Synchroton Radiat. News* **2002**, *15*, 35−42.
(27) Papadakis, C. M.; Di, Z.; Posselt, D.; Smilgies, D.-M. *Langmuir* **2008**, *24*, 13815−13818.
(28) Smilgies, D.-M.; Li, R.; Di, Z.; Darko, C.; Papadakis, C. M.; Posselt, D. *Mater. Res. Soc. Symp. Proc.* **2009**, *1147*, OO01−01.
(29) Di, Z.; Posselt, D.; Smilgies, D.-M.; Papadakis, C. M. *Macromolecules* **2010**, *43*, 418−427.
(30) Di, Z.; Posselt, D.; Smilgies, D.-M.; Li, R.; Rauscher, M.; Potemkin, I. I.; Papadakis, C. M. *Macromolecules* **2012**, *45*, 5185−5195.
(31) Hoogerbrugge, P. J.; Koelman, J. M. V. A. *Europhys. Lett.* **1992**, *19*, 155−160.
(32) Koelman, J. M. V. A.; Hoogerbrugge, P. J. *Europhys. Lett.* **1993**, *21*, 363−368.
(33) Groot, D.; Warren, P. B. *J. Chem. Phys.* **1997**, *107*, 4423−4435.
(34) Pagonabarraga, I.; Hagen, M. H. J.; Frenkel, D. *Europhys. Lett.* **1998**, *42*, 377−382.
(35) Zhulina, E. B.; Birshtein, T. M. *Polym. Sci.* **1987**, *29*, 1678.
(36) Semenov, A. N. *Sov. Phys. JETP* **1985**, *61*, 733−742.
(37) Fredrickson, G. H.; Leibler, L. *Macromolecules* **1989**, *22*, 1238−1250.
(38) Glagoleva, A.; Erukhimovich, I.; Vasilevskaya, V. *Macromol. Theory Simul.* **2013**, *22*, 31−35.
(39) Papadakis, C. M.; Almdal, K.; Mortensen, K.; Posselt, D. *Europhys. Lett.* **1996**, *36*, 289.
(40) Burrell, H. In *Polymer Handbook*, 2nd ed.; Brandrup, J., Immergut, E. H., Eds.; Wiley & Sons: New York, 1975; p IV/337 ff.
(41) Busch, P.; Rauscher, M.; Smilgies, D.-M.; Posselt, D.; Papadakis, C. M. *J. Appl. Crystallogr.* **2006**, *39*, 433.
(42) Salditt, T.; Münster, C.; Lu, J.; Vogel, M.; Fenzl, W.; Souvorov, A. *Phys. Rev. E* **1999**, *60*, 7285.
(43) Gutmann, J. S.; Müller-Buschbaum, P.; Schubert, D. W.; Stribeck, N.; Smilgies, D.; Stamm, M. *Physica B* **2000**, *283*, 40.